JOURNAL OF MATERIALS SCIENCE 29 (1994) 645–651

Diffusion controlled growth or dissolution of long cylindrical particles

J. R. FRADE
Departamento de Engenharia Cerâmica e do Vidro, Universidade de Aveiro, 3800 Aveiro, Portugal

The analytical solutions for growth from zero initial radius of long cylindrical particles are extended to include arbitrary changes in volume. These analytical solutions are used to demonstrate the accuracy of numerical solutions required to obtain solutions for dissolution and for the initial stage of growth from finite initial size.

1. Introduction

Radial growth or shrinkage of fibres may occur during the processing of materials, which includes the development of superlattice-type structures, phase transformations in covalent ceramics, etc. These processes often involve both diffusion and heat conduction, and may be closely approximated by cylindrical symmetry [1, 2]. The present work describes diffusion-controlled growth or dissolution, assuming uniform temperature. However, diffusive mass transfer and heat conduction are described by similar dimensionless solutions for many processes described by one-, two- or three-dimensional equations. The radially symmetrical behaviour of cylinders requires consideration of two dimensions, which often makes them more complex than for plane layers or spherical symmetry. For example, the analytical solutions for diffusion in a plane layer or in the medium internally bounded by a sphere are easily computed from the error function $\mathrm{erf}(x)$ [3]; this is not the case for diffusion in a medium internally bounded by a cylinder. Nevertheless, some solutions for growth from zero apply to one-, two- and three-dimensional processes [4, 5]. The solutions for spherical symmetry have also been extended to include changes in volume for different partial molar volumes in the matrix and in the particle [6].

A number of numerical solutions have also been reported for the diffusion-controlled behaviour of spheres [7–15]. In contrast, numerical solutions for cylindrical symmetry are rare [1]. Kim and Yue [1] did not take into account the effects of volume changes or moving boundaries. Analytical solutions for growth from zero may also be useful to assess the accuracy of numerical methods, as previously shown for spherical symmetry [11–13].

Relatively simple quasi-steady-state approximations have also been obtained for the diffusion-controlled behaviour of spheres, for both finite and infinite matrices. On the other hand, steady-state or quasi-steady-state solutions for cylindrical symmetry can only be obtained if the matrix is finite (hollow cylinder) [3]; this restriction has not been properly recognized [16]. A quasi-steady-state solution for diffusion in a finite cylindrical layer was obtained by Valensi [17] to describe the diffusion-controlled oxidation of metallic wires; this has now been extended (see Appendix B). The applicability can be assessed by comparison between quasi-steady-state and exact solutions for growth from zero, or comparison between quasi-steady-state and numerical solutions.

2. Theory

2.1. Formulation

An isolated cylinder is assumed to be surrounded by an infinite matrix in which the only convective flow is the radial velocity that must occur if the diffusing species or solute has different partial molar volumes in the particle and in the matrix; this flow is assumed to occur without hindrance. Diffusion in the matrix is assumed to control the mass transfer across the interface, equilibrium being maintained at the interface. Interfacial energy is also assumed to have a negligible effect on interfacial conditions. The cylinder is assumed uniform in composition, with constant properties; this is also assumed for the initial properties and composition of the matrix. The partial molar volumes in the matrix are assumed constant, but do not need to be the same for solute and solvent. Therefore

$$\sum_{i=1}^{n} y_i = \sum_{i=1}^{n} C_i v_i = 1 \tag{1}$$

where y_i is the volume fraction of species i, C_i is the molar concentration and v_i is the partial molar volume.

Changes in volume at the interface may give rise to a volume average velocity U, which includes a contribution for every component:

$$U = \sum_{i=1}^{n} U_i y_i \tag{2}$$

The velocity U_i includes the effects of diffusion and radial convection. Therefore, continuity for cylindrical symmetry requires

$$\frac{\partial C_i}{\partial t} + \frac{1}{r}\left(\frac{\partial (r U_i C_i)}{\partial r}\right) = 0 \tag{3}$$

0022–2461

where r is radial distance and t is time. Combination of Equations 1, 2 and 3 leads to

$$U(r) = \frac{a}{r}U(a) \quad (4)$$

where a is the radius of the cylinder.

If a single solute (species 1) crosses the interface between the cylinder and the matrix, its flux is related to the difference between the velocity of solute and that of the interface by

$$C_c\frac{da}{dt} = C_1(a)\left(\frac{da}{dt} - U_1(a)\right) \quad (5)$$

where C_c is the concentration in the cylinder. Transfer of the remaining components is assumed to cancel at the interface, which requires $U_i = da/dt$, for $i \neq 1$. Therefore, from Equations 2 and 5

$$U(a) = \varepsilon\frac{da}{dt} \quad (6)$$

where ε is defined as

$$\varepsilon = 1 - C_c v_1 \quad (7)$$

Note that $C_c v_1$ represents the ratio between the partial molar volumes in the matrix and in the cylinder. Therefore, radial convection will occur and must be considered if ε is significantly different from zero.

Diffusion can also be related to differences between the average velocity and the velocity of solute by

$$D\frac{\partial C_1}{\partial r} = C_1(U - U_1) \quad (8)$$

where D is the diffusion coefficient. Combination of Equations 3, 4, 6 and 8 thus gives the material balance, and the change in radius is given by Equations 5 to 8:

$$\frac{\partial C}{\partial t} = D\frac{\partial^2 C}{\partial r^2} + \left[\frac{D}{r} - \frac{\varepsilon a}{r}\left(\frac{da}{dt}\right)\right]\frac{\partial C}{\partial r} \quad (9)$$

$$\frac{da}{dt} = \frac{D}{C_c[1 - vC(a)]}\left(\frac{\partial C}{\partial r_a}\right) \quad (10)$$

where the index 1 (for solute) was dropped. Uniform initial conditions and constant boundary conditions correspond to

$$C(a, t) = C_a \quad (11)$$

$$C(\infty, t) = C_\infty \qquad C(r, 0) = C_\infty \quad (12)$$

2.2. Growth from zero

Equation 9 is a generalized material balance for moving boundaries. Frank's solutions for growth from zero [5] are true only for very slow motion of the interface, or for nearly unit ratio between the partial molar volumes of solute in the cylindrical phase and in the surrounding matrix. However, the transformation of variables used by Frank [5] and other authors [6, 12, 13] can be used to obtain solutions for Equation 9. On assuming

$$s = \frac{r}{(4Dt)^{1/2}} \quad (13)$$

$$a = 2\beta(Dt)^{1/2} \quad (14)$$

Equation 9 leads to the following ordinary differential equation:

$$\frac{d^2C}{ds^2} + \frac{1 - 2\varepsilon\beta^2}{s}\left(\frac{dC}{ds}\right) = -2s\frac{dC}{ds} \quad (15)$$

with the required boundary conditions

$$C(\beta) = C_a; \qquad C(\infty) = C_\infty \quad (16)$$

Transformation of Equation 10 gives the concentration gradient at the interface as

$$\left(\frac{dC}{ds}\right)_\beta = 2\beta[C_c(1 - vC_a)] \quad (17)$$

The analytical solutions for growth constant β are now obtained by integration of Equation 15:

$$\frac{C - C_a}{C_c(1 - C_a v)} = \int_{a/r}^{1} \exp[\beta^2(1 - x^{-2}) + (1 - 2\varepsilon\beta^2)\ln x]x^{-2}\,dx \quad (18)$$

$$\phi = \int_0^1 x^{-2}\exp[\beta^2(1 - x^{-2}) + (1 - 2\varepsilon\beta^2)\ln x]\,dx \quad (19)$$

$$\phi = \frac{C_\infty - C_a}{C_c(1 - C_a v)} \quad (20)$$

The growth constant β is a function of a dimensionless driving force ϕ, and the volume change parameter ε. Runge–Kutta or multi-step methods can be used to solve Equation 19. Sequential selection of δx increments is useful to ensure that solutions will be stable and convergent, without undue computing time. The selection of δx increments was based on the derivative

$$\delta x_i \leqslant \frac{0.0025x_i^2}{\exp[\beta^2(1 - x_i^{-2}) + (1 - 2\varepsilon\beta^2)\ln x_i]}$$

with an additional restriction $\delta x_i \leqslant 0.0025$.

Table I contains a large number of solutions which can be used to predict growth rates for a very broad range of experimental conditions. The solutions for small ϕ become nearly independent of volume changes, but growth constants β increase rapidly as ϕ tends to $1/(1 - \varepsilon)$; this demonstrates the importance of volume changes. The effect of volume changes is related to a contribution by radical convection, which enhances the rate of transfer for net volume decrease ($\varepsilon < 0$). However, radial convection has the opposite effect when there is an increase in volume ($\varepsilon > 0$).

2.3. Growth from finite size

The solutions for growth from zero (Equations 14 and 19) fail for a transient stage of growth from finite size although they represent the asymptotic behaviour. Alternative solutions are thus needed for the transient stage. Note that experimental data usually correspond to a relatively small increase in size $a_0 \leqslant a < 2a_0$, which may therefore fall in the transient regime. The finite difference method is described in Appendix A. This method was also used to obtain solutions for dissolution.

TABLE I Solutions for growth from zero (Equation 19)

β	$\phi(\beta, \varepsilon)$						
	$\varepsilon = -0.5$	$\varepsilon = -0.25$	$\varepsilon = -0.1$	$\varepsilon = 0$	$\varepsilon = 0.1$	$\varepsilon = 0.25$	$\varepsilon = 0.5$
0.01				0.000 863			
0.012				0.001 190			
0.015				0.001 760			
0.02				0.002 899			
0.025				0.004 253			
0.03	0.005 79	0.005 79	0.005 80	0.005 80	0.005 80	0.005 80	0.005 81
0.04	0.009 37	0.009 38	0.009 39	0.009 39	0.009 40	0.009 40	0.009 42
0.05	0.013 53	0.013 55	0.013 57	0.013 58	0.013 58	0.013 60	0.013 62
0.07	0.023 22	0.023 30	0.023 34	0.023 37	0.023 40	0.023 44	0.02352
0.1	0.040 34	0.040 56	0.040 70	0.040 78	0.040 88	0.041 01	0.041 24
0.12	0.040 34	0.040 56	0.040 70	0.040 78	0.040 88	0.041 01	0.041 24
0.15	0.073 02	0.073 78	0.074 24	0.074 50	0.074 86	0.075 33	0.076 11
0.2	0.1082	0.1099	0.1109	0.1116	0.1123	0.1134	0.1153
0.25	0.1438	0.1469	0.1488	0.1502	0.1515	0.1535	0.1570
0.3	0.1787	0.1837	0.1868	0.1889	0.1911	0.1944	0.2001
0.4	0.2440	0.2540	0.2603	0.2646	0.2690	0.2759	0.2878
0.5	0.3016	0.3177	0.3281	0.3352	0.3426	0.3542	0.3748
0.7	0.3933	0.4235	0.4434	0.4577	0.4724	0.4962	0.5400
1	0.4843	0.5355	0.5707	0.5963	0.6239	0.6694	0.7579
1.2	0.5240	0.5874	0.6320	0.6650	0.7010	0.7613	0.8827
1.5	0.5644	0.6427	0.6993	0.7421	0.7896	0.8711	1.043
2	0.6031	0.6985	0.7700	0.8254	0.8883	1.000	1.250
2.5	0.6238	0.7300	0.8115	0.8757	0.9498	1.085	1.402
3	0.6360	0.7492	0.8374	0.9078	0.9900	1.142	1.516
4	0.6489	0.7701	0.8662	0.9441	1.037	1.212	1.668
5	0.6551	0.7804	0.8808	0.9629	1.061	1.251	1.762
7	0.6607	0.7898	0.8942	0.9804	1.084	1.288	1.862
10	0.6637	0.7949	0.9017	0.9902	1.098	1.311	1.927
12	0.6646	0.7965	0.9039	0.9932	1.102	1.317	1.948
15	0.6654	0.7977	0.9058	0.9956	1.105	1.323	1.966
20	0.6659	0.7987	0.9072	0.9975	1.108	1.327	1.980
25	0.6662	0.7992	0.9079	0.9984	1.109	1.330	1.987
30	0.6663	0.7994	0.9083	0.9989	1.110	1.331	1.991
40	0.6665	0.7997	0.9086	0.9994	1.110	1.332	1.995
50	0.6665	0.7998	0.9088	0.9996	1.111	1.332	1.997
70	0.6666	0.7999	0.9089	0.9998	1.111	1.333	1.998
100	0.6666	0.7999	0.9090	0.9999	1.111	1.333	1.999

The accuracy of the numerical method is demonstrated in Table II for large ranges of the relevant parameters ϕ and ε. The differences between the numerical predictions and the corresponding exact solutions are usually less than 0.2%. $\beta_n = a/(4Dt)^{1/2}$ is the numerical asymptotic solution for a very large increase in size (up to $a/a_0 = 10^5$), and $\phi(\beta_n, \varepsilon)$ is the exact solution for growth from zero (Equation 19).

Figs 1 to 3 compare growth from zero and finite initial size plotted against dimensionless time in three different forms. Fig. 2 shows the obvious plot against dimensionless time but introducing the factor 2β; Fig. 2 gives a common asymptote for all solubilities (ϕ) although the value of ϕ still affects initial growth. However, the form used in Fig. 3 shows that the asymptotic behaviour (Table I) may be used for a very wide range of solubilities and size greater than twice the initial value if a different time dependence is employed:

$$a = (4\beta^2 Dt + a_0^2)^{1/2} \quad (21)$$

For very small ϕ, this dependence is nearly true from the beginning. In addition, some transient effects may also account for a slower initial stage, which contributes to minimizing the differences between the actual solutions and Equation 21. For example, the interfacial energy may cause decrease in driving-force for growth.

2.4. Dissolution

Figs 4–6 show normalized dissolution curves. The shape of these curves is sensitive to the value of ϕ, especially in the intermediate range, which may be useful for evaluating both ϕ and the diffusion coefficient D from experimental data. However, such an exercise should avoid using data for the final stage ($a < 0.1a_0$) because that stage may well be influenced by interfacial energy which can accelerate the last stage of dissolution.

Differences in partial molar volumes in the particle and matrix may contribute to radial convection towards the interface, for decrease in volume ($\varepsilon > 0$), or outwards radial convection, for increase in volume ($\varepsilon < 0$). The increase in dissolution times with decreasing ε is due to this effect, especially for large $|\phi|$ (Table III). However, outwards radial convection during the initial stage may also retard solute accumulation when the volume of the particle has decreased to a small fraction of its initial value, especially for large

TABLE II Comparison between numerical solutions of partial differential Equation 9, $\beta_n = a/(4Dt)^{1/2}$, for up to $a/a_0 = 10^5$, and analytical solutions for growth from zero $\phi(\beta_n, \varepsilon)$ (Equation 19)

ϕ	$\varepsilon = 0$		$\varepsilon = 0.5$		$\varepsilon = -0.5$	
	β_n	$\phi(\beta_n, \varepsilon)$	β_n	$\phi(\beta_n, \varepsilon)$	β_n	$\phi(\beta_n, \varepsilon)$
0.01	0.041 57	0.010 01	0.041 49	0.010 01	0.041 62	0.010 01
0.10	0.1847	0.1001	0.1811	0.1001	0.1886	0.1000
0.20	0.3146	0.2001	0.3001	0.2002	0.3317	0.2002
0.50	0.782	0.501	0.650	0.5005	1.075	0.5007
0.65					4.148	0.650
0.75	1.542	0.751				
0.90	2.883	0.901				
0.95	4.311	0.951				
0.99	9.23	0.989				
1.00			1.417	1.001		
1.50			2.932	1.502		
1.90			8.53	1.902		

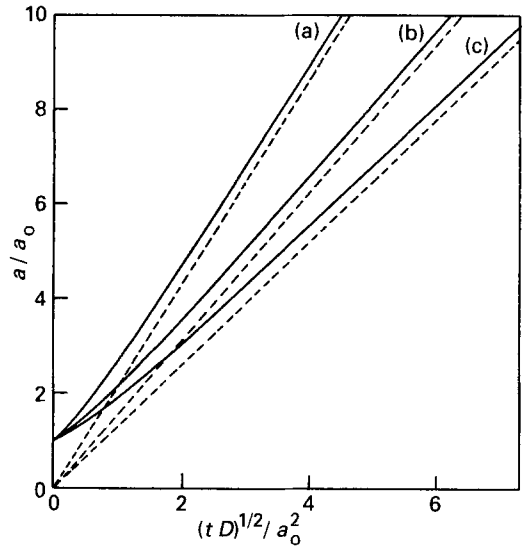

Figure 1 Growth from finite size (full lines) for ε = (a) −0.5, (b) 0 and (c) 0.5 with $\phi = 0.5$. The dashed lines represent the corresponding solutions for growth from zero (Equations 14 and 19).

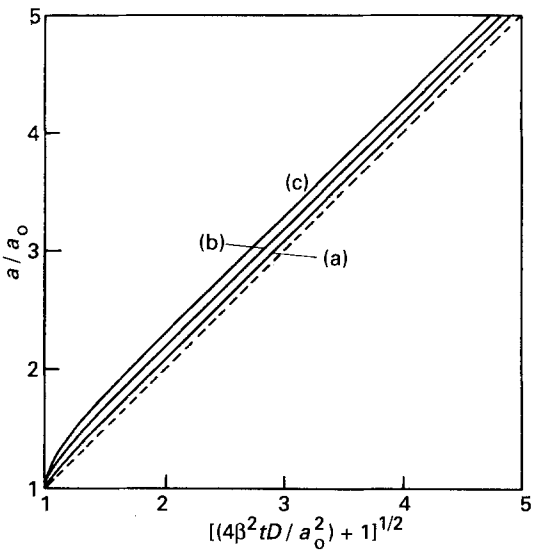

Figure 3 Growth from finite size for ϕ = (a) 0.001, (b) 0.1 and (c) 0.5 with $\varepsilon = 0$. The dashed line represents Equations 14 and 19.

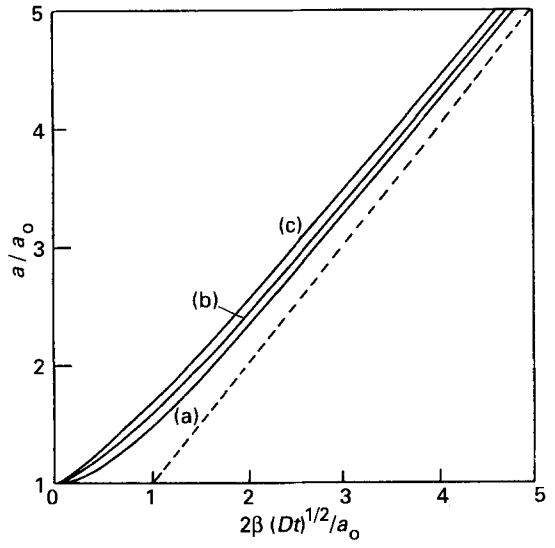

Figure 2 Growth from finite size for ϕ = (a) 0.001, (b) 0.1 and (c) 0.5 with $\varepsilon = -0.5$. The dashed line represents growth from zero (Equations 14 and 19).

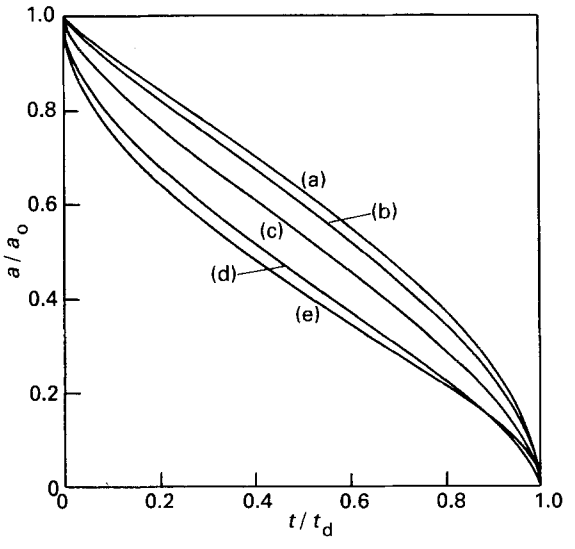

Figure 4 Normalized dissolution curves for $-\phi$ = (a) 0.001, (b) 0.01, (c) 0.1, (d) 1 and (e) 10 with $\varepsilon = -0.5$.

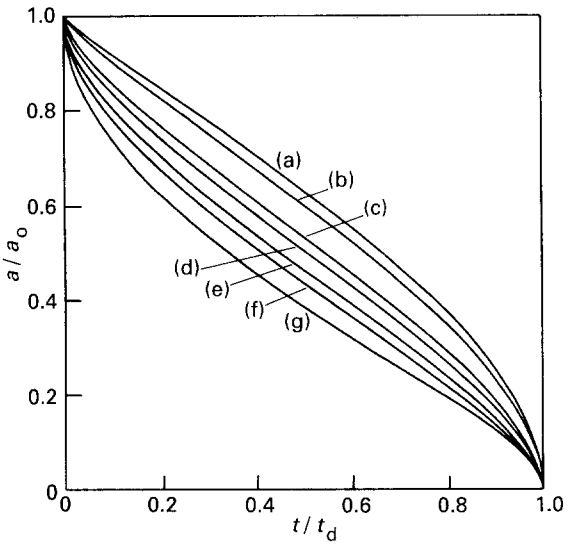

Figure 5 Normalized dissolution curves for $-\phi$ = (a) 0.001, (b) 0.01, (c) 0.1, (d) 0.2, (e) 0.5, (f) 1 and (g) 10 with $\varepsilon = 0$.

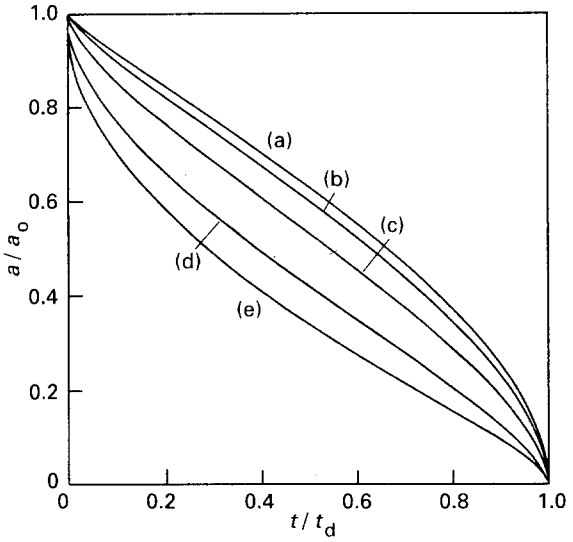

Figure 6 Normalized dissolution curves for $-\phi$ = (a) 0.001, (b) 0.01, (c) 0.1, (d) 1 and (e) 10 with $\varepsilon = 0.5$.

$|\phi|$; this may allow faster dissolution during the final stage (Fig. 4). Note that the residual volume is 1% for $a = 0.1a_0$.

2.5. Limitations of quasi steady state solutions

Steady-state or quasi-steady-state solutions are simple and commonly used. The solutions for diffusion-controlled growth of a long cylinder are derived in Appendix B for a finite matrix. The simplest case is for $\varepsilon = 0$, which reduces to

$$(a^2 - a_0^2)\left(\ln B + \frac{1}{2}\right) - a^2 \ln\left(\frac{a}{a_0}\right) = 2\phi Dt \qquad (22)$$

where $B = b_0/a_0$ is the radial ratio between the outer boundary of the matrix and the cylinder. This method fails for an infinite matrix with cylindrical symmetry, because there is no finite limit for factor $\ln B$. This limitation is also true for one-dimensional diffusion in semi-infinite media, which cannot be described by steady-state or quasi-steady-state solutions. On the other hand, spherical symmetry may be described by steady-state solutions for both finite and infinite media [11, 13].

TABLE III Dimensionless times required for complete dissolution

$-\phi$	$t_d D/a_0$		
	$\varepsilon = -0.5$	$\varepsilon = 0$	$\varepsilon = 0.5$
0.001	2177	2176	2175
0.01	155.9	155.4	154.9
0.1	10.22	9.91	9.59
0.2	4.58	4.32	4.05
0.5	1.711	1.512	1.310
1	0.897	0.742	0.582
10	0.2062	0.1413	0.0763

3. Conclusions

A revised formulation of the relevant material balances was found suitable for extending the range of analytical solutions for two-dimensional diffusion-controlled growth; this includes volume changes. Exact analytical solutions describe growth from zero initial radius. These asymptotic solutions were found useful to demonstrate the accuracy of numerical methods required for transient regimes, i.e. dissolution or growth from finite size. A transient stage for growth from finite size usually reduces to the time required to double the initial size or shorter, when a suitable time dependence is used. The quasi-steady-state solutions fail for large matrices.

The solutions for very small driving force $|\phi|$ are nearly independent of volume changes. In constrast, volume changes are very effective for large $|\phi|$; this is true for both dissolution and growth.

Acknowledgements

The University of Aveiro allowed sabbatical leave of absence at the University of California, Los Angeles USA, where this work was performed. The Calouste Gulbenkian Foundation is thanked for additional financial support.

Appendix A: Finite difference method

Dimensionless variables were used to minimize the number of parameters required to obtain solutions for growth from finite size or dissolution. The relevant variables are a dimensionless time τ, a space variable which immobilizes the boundary, and a modified concentration function $F(C, x)$ which assists the convergence of the method. We have

$$x = r/a \qquad (A1)$$

$$\tau = tD/a_0^2 \qquad (A2)$$

$$F = \frac{(r/a)^{1/2}(C - C_\infty)}{C_s(1 - C_a v)} \qquad (A3)$$

Equations 9 and 10 are thus transformed to give

$$R^2\frac{\partial F}{\partial \tau} = \frac{\partial^2 F}{\partial x^2} + \frac{x-(\varepsilon/x)}{2}\left(\frac{d(R^2)}{d\tau}\right)\frac{\partial F}{\partial x} + \frac{d(R^2)}{d\tau}[\varepsilon x^{-2} - 1 + x^{-2}]\frac{F}{4} \quad \text{(A4)}$$

$$\frac{d(R^2)}{d\tau} = 2\frac{\partial F}{\partial x_1} + \phi \quad \text{(A5)}$$

$$F(1,\tau) = -\phi \quad F(\infty,\tau) = 0 \quad F(x,0) = 0 \quad \text{(A6)}$$

An implicit finite-difference algorithm [18] was used to solve Equation A4. The concentration gradient and the change in radius (Equation A5) were computed from the first three radial mesh points at time τ_{j-1}:

$$\left(\frac{\partial F}{\partial x}\right)_1 = \frac{2F_2 - 1.5F_1 - 0.5F_3}{\delta x} \quad \text{(A7)}$$

This was corrected after computing a new concentration profile for time τ_j.

Radial mesh points were redistributed every 15 time steps. Radial mesh sizes δx were equal in a range $1 < x < 1 + \delta_D$, and allowed to increase with distance; $\delta x_i = 1.1\delta x_{i-1}$ for $x > 1 + \delta_D$. δ_D corresponds to the boundary layer thickness:

$$\delta_D = \left|\frac{\phi}{(\partial F/\partial x)_1}\right| \quad \text{(A8)}$$

$$\delta x = (x_i - x_{i-1}) = \delta_D/n_1 \quad i = 2,\ldots,n_1 \quad \text{(A9)}$$

$$\delta x_i = 1.1\delta x_{i-1} \quad i = n_1 + 1,\ldots,n_2 \quad \text{(A10)}$$

$$x_0 = 1 \quad \text{(A11)}$$

Truncation was also used for $x_{n2} \geqslant 1 + 100\delta_D$, with an additional restriction $x_{n2} \geqslant 1 + 1/|\phi|$ for very small $|\phi|$. The numerical solutions are not significantly changed by using truncation for larger distances.

Formulae for radial derivatives were derived from a truncated series expansion; this gives standard formulae [18] for the range where mesh points are equally spaced and $1 \leqslant x \leqslant 1 + \delta_D$. However, modified formulae are needed for $x > 1 + \delta_D$, where $\delta x_{i+1} = 1.1\delta x_i$:

$$\frac{\partial F}{\partial x_i} = \frac{F_{i+1} - 1.21F_{i-1} + 0.21F_i}{2.31\delta x_i} \quad \text{(A12)}$$

$$\frac{\partial^2 F}{\partial x_i^2} = \frac{2F_{i+1} - 4.2F_i + 2.2F_{i-1}}{2.31(\delta x_i)^2} \quad \text{(A13)}$$

The time increments were also adjusted after every time step to control the changes in radius a and the increase in boundary layer thickness per time step. These criteria correspond to

$$\delta\tau \leqslant \frac{0.01R}{|dR/d\tau|} \quad \text{(A14)}$$

$$\delta\tau \leqslant 0.015\tau \quad \text{(A15)}$$

The stability and convergence of this numerical method were assessed by making the radial and time mesh sizes smaller and seeing when the effects became negligible. The condition is true for $n_1 = 100$ (see Equations A9 and A10) and for Equations A14 and A15, used to control the time mesh sizes. Sequential control adjusts radial and time mesh sizes to the actual radius of the cylinder, which is required for computing a very large increase in size without excessive computing time. For example, increases in size by five orders of magnitude ($a = 10^5 a_0$) corresponds to an increase in time scale by a factor of 10^{10}; this was easily computed by using the variable criteria of Equations A14 and A15, but cannot be dealt with if a constant mesh size is used. Note also that for $a > 10^3$ the effect of a finite initial size becomes negligible, and the accuracy of numerical solutions could be assessed by comparison between numerical solutions for growth from finite initial size and exact asymptotic solutions for growth from zero.

Appendix B: quasi steady state solutions for a finite matrix

The solutions for a finite matrix are easily obtained from quasi-steady-state requirements; these are $\partial C/\partial t \simeq 0$, and very slow motion of the interface. If $r = b$ is the outer boundary, Equation 9 gives

$$\left(\frac{dC}{dr}\right)_a = \frac{C_\infty - C_a}{a\ln(b/a)} \quad \text{(B1)}$$

which can be combined with Equation 10 to give

$$\frac{da}{dt} = \frac{D(C_\infty - C_a)}{C_c(1 - C_a v)a\ln(b/a)} \quad \text{(B2)}$$

Equations 4 and 6 relate the outer boundary $r = b$ to the change in radius of the cylinder, which gives $d(b^2) = \varepsilon d(a^2)$. Therefore, integration of Equation B2 gives

$$(R^2 - 1)\left[2\ln B + \ln\left(1 + \frac{\varepsilon(R^2-1)}{B^2}\right)\right] - 2R^2\ln R + \frac{B^2}{\varepsilon}\ln\left(1 + \frac{\varepsilon(R^2-1)}{B^2}\right) = \frac{4\phi Dt}{a_0^2} \quad \text{(B3)}$$

where $B = b_0/a_0$, $R = a/a_0$ and, $\varepsilon = 1 - vC_c$. The simplest case is for $\varepsilon = 0$, when $b = b_0$ is constant:

$$(a^2 - a_0^2)\left(\ln B + \frac{1}{2}\right) - a^2\ln\left(\frac{a}{a_0}\right) = 2\phi Dt \quad \text{(B4)}$$

The solution obtained by Valensi [17] for the diffusion-controlled corrosion of metallic wires corresponds to $B = 1$ and $\varepsilon = 0$, which is the simplest case. On the other hand, for a large size ration B, $\varepsilon(R^2 - 1)/B^2 \ll 1$, and Equation B3 then reduces to

$$(R^2 - 1)(1 + 2\ln B) - 2R^2\ln R = \frac{4\phi Dt}{a_0^2} \quad \text{(B5)}$$

References

1. B. Y. KIM and A. S. YUE, *J. Cryst. Growth* **79** (1986) 874.
2. V. K. PINUS and P. L. TAYLOR, *Phys. Rev. B* **32** (1985) 5362.
3. J. CRANK, "The Mathematics of Diffusion", 2nd Edn. (Clarendon, Oxford, 1979) p. 69, 89.
4. C. ZENER, *J. Appl. Phys.* **20** (1949) 950.
5. F. C. FRANK, *Proc. Roy. Soc.* **A201** (1950) 586.
6. L. E. SCRIVEN, *Chem. Eng. Sci.* **10** (1959) 1.
7. D. W. READEY and A. R. COOPER, *ibid.* **21** (1966) 917.
8. M. CABLE and D. J. EVANS, *J. Appl. Phys.* **38** (1967) 2899.
9. J. L. DUDA and J. S. VRENTAS, *A.I.Ch.E.J.* **15** (1969) 351.
10. *Idem, J. Heat Mass Transfer* **14** (1971) 395.
11. M. CABLE and J. R. FRADE, *J. Mater. Sci.* **22** (1987) 149.
12. *Idem, ibid.* **22** (1987) 919.
13. *Idem, Chem. Eng. Sci.* **42** (1987) 2525.
14. J. SZEKELY and G. P. MARTINS, *ibid.* **26** (1971) 147.
15. J. SZEKELY and S. D. FANG, *ibid.* **28** (1973) 2127.
16. O. SIMMICH and H. LOFFLER, *Phys. Status Solidi.* **65** (1981) 153.
17. G. VALENSI, *C R. Acad. Sci.* **201** (1935) 602.
18. G. D. SMITH, "Numerical Solutions of Partial Differential Equations: Finite Difference Methods, 2nd Edn (Oxford University Press, Oxford, 1978) 11.

Received 28 May 1992
and accepted 20 August 1993